Conformational Distribution of a Multi-Domain Protein Measured by Single-Pair Small Angle X-Ray Scattering

Honoka Kawamukai[1,2], Shumpei Takishita[1], Kazumi Shimizu[3], Daisuke Kohda[4],

Koichiro Ishimori[1,5], and Tomohide Saio*[2,6,7]*

1. Graduate School of Chemical Sciences and Engineering, Hokkaido University, Sapporo, Hokkaido 060-8628, Japan

2. Graduate School of Medical Sciences, Tokushima University, Tokushima 770-8503, Japan

3. Faculty of Education and Integrated Arts and Sciences, Waseda University, Tokyo 169-8050, Japan

4. Division of Structural Biology, Medical Institute of Bioregulation, Kyushu University, Fukuoka 812-8582, Japan

5. Department of Chemistry, Faculty of Science, Hokkaido University, Sapporo, Hokkaido 060-0810, Japan

6. Institute of Advanced Medical Sciences, Tokushima University, Tokushima 770-8503, Japan

7. Fujii Memorial Institute of Medical Sciences, Institute of Advanced Medical Sciences, Tokushima University, Tokushima 770-8503, Japan

Corresponding Author

Koichiro Ishimori
Email: koichiro@sci.hokudai.ac.jp.

Tomohide Saio
Email: saio@tokushima-u.ac.jp.

ABSTRACT

The difficulty in evaluating the conformational distribution of proteins in solution often hinders mechanistic insights. One possible strategy for visualizing conformational distribution is distance distribution measurement by single-pair small-angle X-ray scattering (SAXS), in which the scattering interference from only a specific pair of atoms in the target molecule is extracted. Despite this promising concept, with few applications in synthetic small molecules and DNA, technical difficulties have prevented its application in protein conformational studies. This study used a synthetic tag to fix the lanthanide ion at desired sites on the protein and used single-pair SAXS with contrast matching to evaluate the conformational distribution of the multi-domain protein enzyme MurD. These data highlighted the broad conformational and ligand-driven distribution shifts of MurD in solution. This study proposes an important strategy in solution structural biology that targets dynamic proteins, including multi-domain and intrinsically disordered proteins.

TOC GRAPHICS

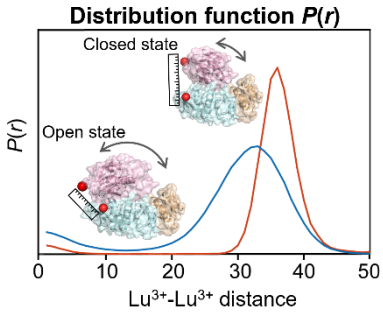

KEYWORDS

42 Single-pair SAXS, protein conformational ensemble, multi-domain protein, contrast-matching,

43 lanthanide ion

44

Conformational distribution is the key to understanding how proteins, especially multi-domain proteins, function in solution. Multi-domain proteins often regulate their activity by changing the population of multiple conformational states with varying domain orientations, contingent on ligand binding, post-translational modifications, and environmental changes[1–4]. However, evaluating the conformational distribution of multi-domain proteins in solution is not straightforward[5,6]. Although recent technical developments in cryo-EM have expanded the application of the method to the structural determination of proteins with conformational variations, its application to those with continuous variations remains challenging. Additionally, the impact of freezing proteins for detection needs to be considered[7]. Solution nuclear magnetic resonance (NMR) is useful for the structural study of proteins in solution, especially with the use of paramagnetic probes[8,9]. On the other hand, NMR often suffers from resonance averaging because of the exchange among multiple conformational states, making data interpretation difficult. Small-angle X-ray scattering (SAXS) is one of the few methods for quantitatively assessing the conformational polydispersity of macromolecules, including multi-domain proteins with flexible linkers and intrinsically disordered proteins (IDPs)[10]. However, the structural information obtained from typical SAXS analysis is of low resolution because each X-ray scattering between all the atom pairs in the protein sums up to make a single SAXS curve; accordingly, the information is averaged. One way to obtain the

63 conformational distribution of a protein is to exploit atoms with higher electron densities than
64 those consisting of proteins. Scattering interference between heavy atoms on the protein can
65 be extracted by contrast-matching[11] or reference subtraction[12,13] to determine the distance
66 distribution between heavy atoms. If heavy atoms are fixed at specific sites on a protein, the
67 distance distribution of the heavy atoms reflects the conformational distribution of the protein.
68 Previous studies using SAXS have demonstrated the measurement of the distance distribution
69 for colloidal gold particles fixed at both ends of double-stranded DNA[12,13]. A limitation was the
70 size of the gold particle, 14 Å. The gold particle size is adequate for measuring the length of
71 10~35 bp DNA, with distance ranging from 50 to 140 Å, but is often too large to assess
72 conformation changes in proteins. A demonstration using smaller particles was reported using
73 two iodine atoms connected by a PEG chain, in which the distance distribution for a single pair
74 of iodine atoms was obtained by reference subtraction[14]. However, single-pair SAXS has not
75 yet been used in protein conformational studies. Although SAXS distance measurements have
76 been demonstrated for a calcium-binding protein substituted with four lead ions, the distance
77 distribution was not obtained in this study presumably because of the complexity of the analysis
78 owing to the four metals, resulting in six possible pair distances[11]. Furthermore, its application
79 is limited to metalloproteins; however, a new strategy applicable to non-metalloproteins is
80 anticipated.

In this study, we evaluated the conformational distribution of a multi-domain protein by single-pair SAXS using Lu^{3+} attached to two specific sites on the protein using a tag. Lu^{3+} has the highest number of electrons among the lanthanide ions; thus, providing a larger X-ray scattering intensity compared to atoms consisting of proteins. Another advantage of lanthanide ions is that the techniques used to fix the ion to a specific site of the target protein have been extensively studied, especially in the field of biomolecular NMR[8]. Among a number of lanthanide-binding tags, we used Caged Lanthanide NMR Probe 5 (CLaNP-5)[15,16] attached to the protein through two arms to reduce the mobility of the tag with respect to the protein; accordingly, this provides more defined and reliable information about domain conformational states. X-ray scattering arising from Lu^{3+} was observed under contrast-matched conditions using 65% aqueous sucrose buffer, whose electron density matched that of the protein, resulting in the suppression of scattering from protein atoms at low angles[11,17].

To demonstrate the conformational analysis of a multi-domain protein using single-pair SAXS, we used a multi-domain protein, MurD. MurD consists of three domains and is one of the ATP-driven Mur ligases responsible for peptidoglycan biosynthesis. Conformational states and ligand-driven conformational changes in MurD have been well-characterized in previous studies using X-ray crystallography, NMR, molecular dynamics (MD) simulations, and electron spin resonance (ESR)[18–23]. This makes MurD one of the best targets to demonstrate the

application of single-pair SAXS. First, we evaluated the integrity of the strategy by distance distribution measurement for the two lutetium ions (both fixed on the same domain of MurD) and confirmed that the result corresponded to the distance estimated from previous studies. Next, we conducted a conformational study of the full-length MurD with lutetium ions in domains 2 and 3. The data showed that MurD exists in multiple open conformations. On the other hand, inhibitor binding eliminates the conformations toward the closed conformation, highlighting the utility of single-pair SAXS for protein conformational studies in solution.

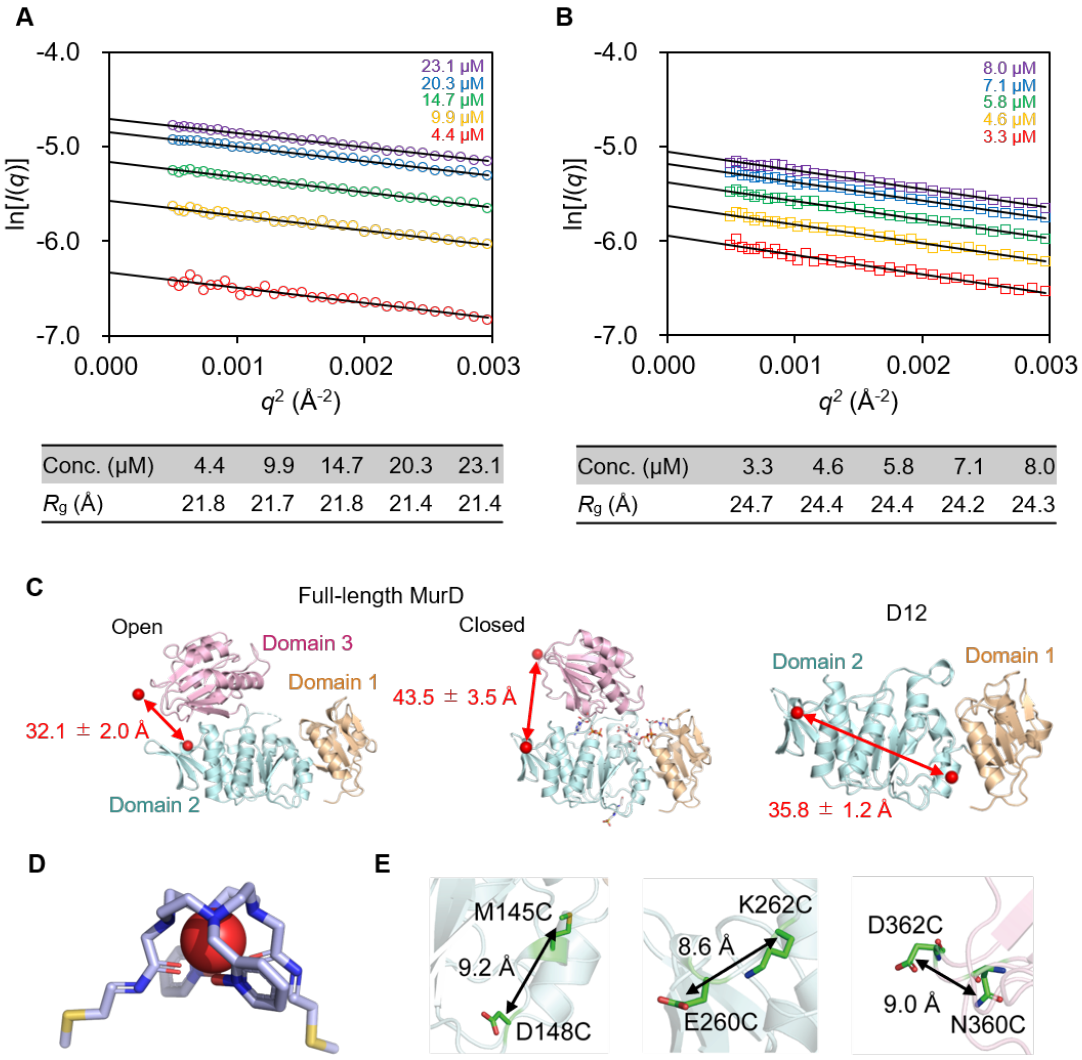

Conc. (µM)	4.4	9.9	14.7	20.3	23.1
R_g (Å)	21.8	21.7	21.8	21.4	21.4

Conc. (µM)	3.3	4.6	5.8	7.1	8.0
R_g (Å)	24.7	24.4	24.4	24.2	24.3

Figure 1. SAXS characterization and construct designs of MurD.

(A, B) Guinier approximation, ln[$I(q)$] vs. q^2, of D12 and MurD scattering data in SEC-SAXS. The straight line gives the slope of data points from the least-squares method.

(C) Lutetium tagging of MurD. The positions of the metals in MurD domains 1–2 M145C/D148C/C151A/E260C/K262C ($D12_{145\text{-}260}$) and MurD E260C/K262C/N360C/D362C ($MurD_{260–360}$) are shown as red spheres in the crystal structures of MurD (PDB:1e0d, 3uag).

Domains 1, 2, and 3 are shown in yellow, blue, and pink, respectively. The distance between the lanthanoid ions, as estimated by crystal structures and pseudocontact shift (PCS) NMR analysis[24] is indicated by a red arrow.

(D) Chemical structure of the Caged Lanthanide NMR Probe 5 (CLaNP-5) tag.

(E) Close-up views of the positions of the lanthanoid ions fixed on MurD. The residues that were mutated to cysteine for ligation with the CLaNP-5 tag are indicated by red sticks.

MurD exists in a dispersed monomeric state

In this study, full-length MurD and MurD domain 1-2 (D12) were used to demonstrate single-pair SAXS. Prior to single-pair SAXS, MurD and D12 were subjected to size exclusion chromatography (SEC)-SAXS to test the oligomeric state and dispersity in solution. SAXS measurements followed by Guinier analysis on D12 and MurD resulted in an R_g of ~21 Å and 23~24 Å, respectively (**Figure 1A**, **1B** and **S1**). The data are consistent with the predicted R_g values of 20.8 Å for D12 and 24.0 Å for MurD as obtained from the crystal structure (PDB ID:1e0d) of the MurD monomer using HullRad[25]. The region comprising residues 1–302 was used to predict the R_g value of D12. The reasonable match between the experimental and predicted R_g values suggests that D12 and MurD exist as stable monomers under SAXS conditions. The monomeric states of D12 and MurD were also corroborated by size-exclusion chromatography with multi-angle light scattering (SEC-MALS), which showed molar mass

values consistent with D12 and MurD existing as monomers (**Figure S2**). Thus, the data showed that D12 and MurD exist as monomers in solution and are suitable for single-pair SAXS.

To investigate the distance distributions of the multi-domain protein MurD, we measured the distance between two lutetium ions fixed on domains 2 and 3 using SAXS (**Figure 1C**). Following the procedures described in previous reports[9,16] pairs of amino acid residues whose C_β atoms are located in a distance of 8–10 Å were selected and mutated to cysteine residues for attachment of CLaNP-5 via disulfide bonds (**Figure 1D** and **1E**). Two MurD variants were constructed for SAXS measurements: MurD domain 1–2 M145C/D148C/C151A/E260C/K262C ($D12_{145\text{-}260}$) and full-length MurD E260C/K262C/N360C/D362C ($MurD_{260–360}$) (**Figure 1C-E**). Because $D12_{145\text{-}260}$ has two Lu^{3+} ions in domain 2, the distance distributions for $D12_{145\text{-}260}$ are expected to reflect the local conformational variation of the tag and the Cys residues bridged to the tag. On the other hand, the distance distribution for $MurD_{260–360}$, with Lu^{3+} ions in domains 2 and 3 was expected to reflect the conformational variations of domain 3 with respect to domain 2, in addition to local conformational variations (**Figure 1C**).

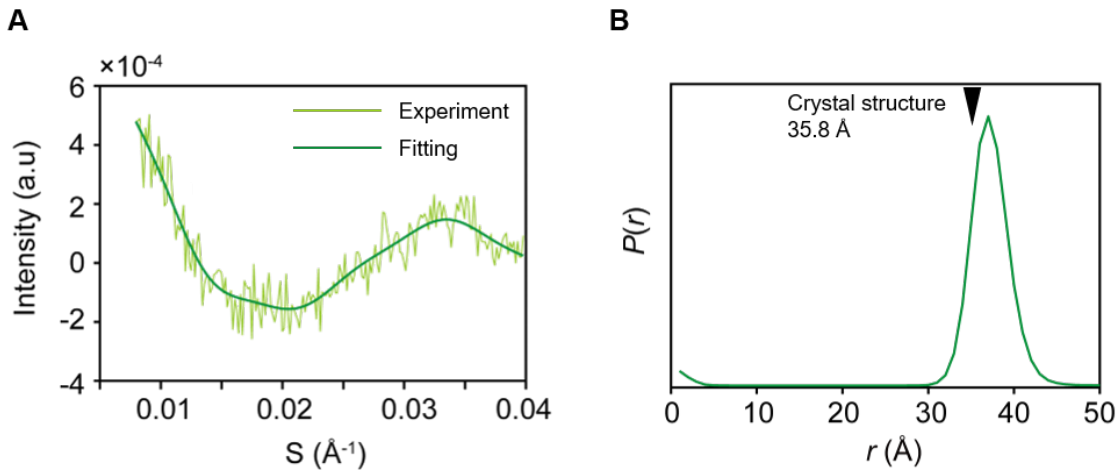

Figure 2. The distance between two points within $D12_{145\text{-}260}$ was measured using flow-SAXS. (A) SAXS scattering data and fitting. (B) Lu^{3+}– Lu^{3+} distance distribution. The arrow indicates the distance between the lutetium ions expected from the crystal structures of MurD domain1-2 (PDB: 3uag, 35.8 Å). The data were analyzed using the MATLAB program.

Single pair SAXS for Lu^{3+}– Lu^{3+}distance measurement on $D12_{145\text{-}260}$

To test whether the inter-lutetium distance information could be extracted, we performed SAXS measurement on $D12_{145\text{-}260}$, in which CLaNP-5 tags containing Lu^{3+} were attached to the rigid regions of domain 2 (**Figure 1C**). To eliminate scattering from protein atoms, we next performed contrast-matched SAXS using a buffer containing 65% sucrose, which has the same electron density as the protein[11]. Prior to contrast-matched SAXS, the effect of 65% sucrose buffer on the structures of D12 and MurD was evaluated using circular dichroism (CD).

Essentially identical CD spectra in the absence and presence of 65% sucrose were observed for D12 and MurD, indicating that the structures of D12 and MurD were preserved, even in 65% sucrose buffer (**Figure S3**).

Contrast-matched SAXS for the $D12_{145\text{-}260}$ data showed an oscillating curve profile characteristic of scattering interference between the two atoms (**Figure 2A**). As a reference experiment, we also obtained the SAXS data for D12 without Lu^{3+} ions (**Figure S4**). Although the data show slightly rugged profile presumably reflecting the non-uniform electron density distribution of the protein[26,27], the disturbance was much less significant compared to the oscillating curve profile for $D12_{145\text{-}260}$ attached with Lu^{3+} ions. The data of the contrast-matched SAXS for $D12_{145\text{-}260}$ attached with Lu^{3+} ions were fitted according to Equation 1:

$$I(q) = {A_e}^2 f^2 \frac{\sin(q.r)}{q.r} \quad (1)$$

where $I(q)$ is the scattering intensity [$q = 4\pi\sin(\theta)/\lambda$, θ = one-half of the scattering angle; λ = X-ray wavelength], A_e is the scattering amplitude of an atom, f is the scattering factor, and r is the atomic distance. The data were fitted using Equation 1 with the maximum entropy procedure coded in MATLAB, which was previously used for the analysis of gold nanocrystal-labeled DNA fragments[12,13]. The fitting using a distance range of 0–200 Å resulted in a major peak around 37 Å, with a couple of minor peaks above 50 Å (**Figure 2B** and **S5A**).

The Lu^{3+}– Lu^{3+} distance on $D12_{145\text{-}260}$ [as estimated from crystal structure and pseudocontact shift (PCS) analysis][9,24] was 35.8 ± 1.2 Å; this agreed with the major peak of SAXS-derived distance distribution curve. Because two Lu^{3+} ions are attached to the same domain, the width of the distribution should be mainly accounted for by the local conformational variation of the tag and the cysteine residues holding the tag. Additionally, the previous study exploiting ESR with double electron-electron resonance (DEER) measurement for $D12_{145\text{-}260}$ showed the distance distribution having a peak top at 36.4 Å and full width at half maximum (FWHM) 7.7 Å[24]; these are highly consistent with the SAXS-derived distance distribution, supporting the reliability of the distance measurement in this method. Note that the minor peaks that appeared in the 50–150 Å range can be explained by intermolecular contributions, given that the average distance between the centers of protein at the concentration of contrast-matched SAXS measurement (700 μM) is estimated as ~130 Å. Thus, the data from contrast-matched SAXS on $D12_{145\text{-}260}$ are highly consistent with the expected values and the results from other measurement techniques; therefore, we concluded that single-pair SAXS using contrast matching successfully extracted the distance distribution of Lu^{3+}– Lu^{3+} on the protein.

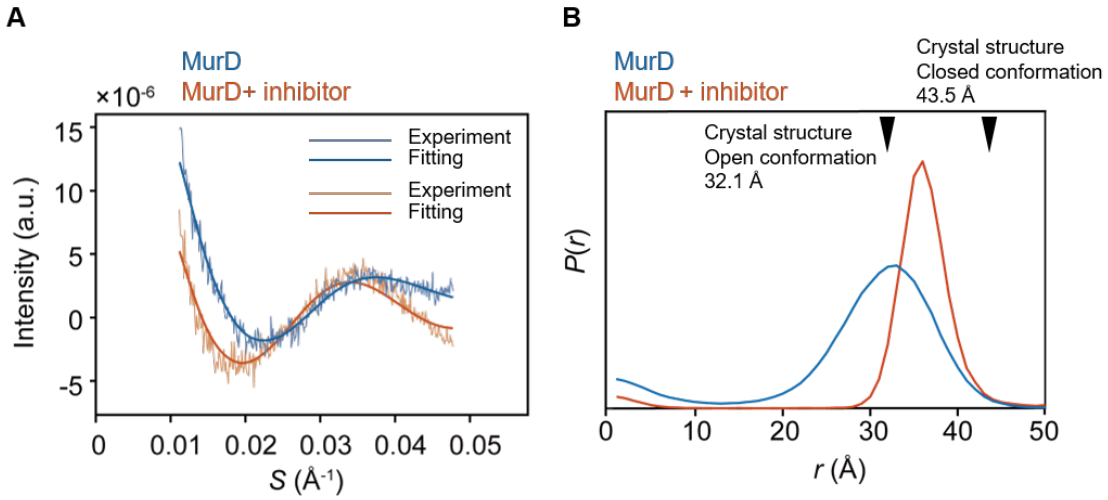

196

197 **Figure 3.** The distance between two points within $MurD_{260–360}$ was measured using flow-SAXS.

198 (A) SAXS scattering data for $MurD_{260–360}$ (blue) and inhibitor-bound $MurD_{260–360}$ (red).

199 (B) Lu^{3+}– Lu^{3+} distance distributions. The insets show a wider distance distribution range of

200 ≤50 Å. The arrows indicate the distance between the lutetium ions expected from the crystal

201 structures of MurD in open (PDB: 1e0d, 32.1 Å) and closed (PDB: 3uag, 43.5 Å)

202 conformations. The data were analyzed using the MATLAB program.

203 Conformational ensemble of MurD investigated by Lu^{3+}– Lu^{3+} single pair SAXS on $MurD_{260-}$

204 $_{360}$

205 The Lu^{3+}– Lu^{3+} distance for $MurD_{260–360}$ was measured to monitor the relative position of

206 domain2 and 3 of MurD in the absence and presence of the inhibitor N-({3-[({4-[(Z)- (2,4-

207 dioxo-1,3-thiazolidin-5-ylidene)methyl]phenyl}amino)methyl]phenyl}carbonyl)-d-glutamic

208 acid[20]. Because the two lutetium ions were attached to domains 2 and 3, the inter-lutetium

distance distribution should reflect the position of domain 3 with respect to domain 2 (**Figure 1C**). The inter-lutetium distance was expected to increase in the closed conformation (**Figure 1C**).

Contrast-matched SAXS of ligand-free $MurD_{260–360}$ resulted in an oscillating SAXS curve, reflecting Lu^{3+}– Lu^{3+} -derived scattering interference (**Figure 3A**). As is the case of $D12_{145-260}$, the data was fitted using Equation 1 with the maximum entropy procedure coded in MATLAB. The fitting resulted in a broader distance distribution peak than that obtained for $D12_{145-260}$ (**Figure 2B and 3B**, blue). The position of the peak top is close to the distance expected from the crystal structure of MurD in the open conformation (PDB:1e0d, 32.1 ± 2.0 Å)[9,22,24] (**Figure 1C**; **3B**, blue), suggesting that MurD exists in a variety of conformational states, including the open conformation seen in the crystal structure as a major state and other associated states.

Contrast-matched SAXS of inhibitor-bound $MurD_{260-360}$ also exhibited an oscillating SAXS curve. Nonetheless, the profile (especially the oscillation frequency and amplitude) was different from that of ligand-free MurD (**Figure 3A**). The fitting resulted in a distance distribution with a major peak at a longer distance and a narrower width compared to ligand-free $MurD_{260-360}$ (**Figure 3B, S5B,** and **S5C**). The narrower width of the peak for inhibitor-bound $MurD_{260–360}$ indicated that inhibitor-bound MurD exists in more defined conformational

226 spaces. The peak position at longer distances in the complex with the inhibitor suggests that
227 the conformation of MurD changed from open to closed.

228 To verify the fitting analysis, theoretical SAXS curves were calculated from the normal
229 distribution, as represented by Equation 2:

230 $$f(x) = \frac{1}{\sqrt{2\pi\sigma^2}} \exp\left(-\frac{(x-\mu)^2}{2\sigma^2}\right) \quad (2)$$

231 where μ is mean of expectation and equals to the peak top of the distance distribution, and σ
232 is standard deviation with the relationship FWHM = 2.35σ. The theoretical SAXS traces
233 corresponding to the distance distributions for $MurD_{260\text{-}360}$ in the absence and presence of the
234 inhibitor (σ = 5.10 Å, μ=33 Å and σ = 2.55 Å, μ=36 Å) replicated the experimental data well
235 (**Figure 3** and **S6**). Next, the reliable range of the distance distribution, apparent distance
236 resolution to distinguish structures, was examined by comparing the experimental and
237 calculated SAXS curves. The experimental SAXS data for $D12_{145\text{-}260}$ were well reproduced by
238 the calculated curve from the normal distribution of the distance corresponding to Figure 2B:
239 μ = 37 Å and σ = 2.12 Å (**Figure S7A** and **B**). The calculated curves with varying μ showed
240 that the those with μ in a range of 37 ± 3 Å fit within the noise level of the experimental data
241 whereas those with μ =37 ± 4 Å protrude from the experimental curve, suggesting that the
242 reliable range of the peak top can be assumed as 37 ± 3 Å. The same evaluation was performed
243 for the data of $MurD_{260\text{-}360}$ in the absence and presence of the inhibitor (**Figure S7C-F**),

resulting the estimated reliable range of the peak top for $MurD_{260\text{-}360}$ in the absence and presence of the inhibitor 33 ± 2 Å and 36 ± 2 Å, respectively. With the above evaluations, we concluded that Lu^{3+}– Lu^{3+} single-pair SAXS allowed us to measure the distance distribution of MurD and inhibitor-induced changes in the distance distribution. Collectively, distance distribution measurements by single-pair SAXS revealed the conformational distribution and ligand-driven conformational changes of the multi-domain protein MurD in solution, thus highlighting the usefulness of this method for evaluating the conformational distribution of proteins in solution.

252 Despite the importance of the conformational distribution of proteins for their function, their
253 evaluation in solution is often not straightforward. This study demonstrates that single-pair
254 SAXS using lanthanide ions as a scattering source can be used to evaluate the distance
255 distribution of a multi-domain protein in solution. Scattering interference between lanthanide
256 ions was selectively observed by suppressing those from protein atoms using contrast-matched
257 SAXS in 65% sucrose buffer. The distance distribution obtained for $D12_{145\text{-}260}$ with the two
258 lanthanide ions in domain 2 showed a major peak with peak top at 37 Å with estimated reliable
259 range of ± 3 Å and was consistent with the distance expected from the crystal structure if the
260 local conformational variation around the tag was considered, indicating the ability of this
261 method to measure the distance between two specific points on the protein (**Figure 2**). Distance
262 measurement for $MurD_{260\text{-}360}$ in the ligand-free state showed a broader distance distribution than
263 that observed for $D12_{145\text{-}260}$, showing a variety of conformational states of MurD. This is
264 consistent with the observations of previous studies using PCS-NMR, ESR, and MD
265 simulation[9,24,28] (**Figure S8**). The position of the peak top, 33 Å with estimated reliable range
266 of ± 2 Å, is also consistent with the crystal structure in the open conformation and previous
267 data from ESR and MD simulation (**Figure 1C** and **S8A**). $MurD_{260\text{-}360}$ in complex with the
268 inhibitor showed a narrower distance distribution at longer distances compared to ligand free
269 $MurD_{260\text{-}360}$, indicating that the inhibitor induces a conformational change toward more closed

and defined conformations. It should be noted that the position of the peak top for inhibitor-bound $MurD_{260–360}$ was located at 36 Å with estimated reliable range of ± 2 Å (**Figure S 7E** and **F**) that is distinct from the crystal structure of MurD in the closed conformation[19] (**Figure 1C**) and the previous ESR distance measurement for frozen protein at 10 K (**Figure S8B**)[24]. These observations suggest the most populated state of inhibitor-bound $MurD_{260-360}$ in solution is different from that seen in the ESR measurement or in the crystal structure. Although the conformational difference of MurD between the crystal and solution has been suggested by other methods (including ESR-DEER measurement[24] and MD simulation[28]), the current data from single-pair SAXS provide the first experimental views of MurD conformation in aqueous solution. However, a current limitation is the difficulty in visualizing the actual conformational state of the inhibitor-bound $MurD_{260-360}$ in solution, mostly because of the limited structural information from distance measurement for a single pair. Further study including the multiple sets of distance measurement for lanthanide ions attached on the other positions would be anticipated.

Using a lanthanide-binding tag, this study successfully demonstrated the application of contrast-matched single-pair SAXS as a tool for visualizing the conformational distribution of a specific protein site. One of the advantages of this strategy is that the distance distribution can be measured for any desired point on the protein as long as the lanthanide can be fixed by

288 the tag. Although we demonstrated the application of the CLaNP-5 tag, the same strategy can
289 be exploited with other lanthanide-binding tags, including single-arm tags for easier design of
290 the fixing points and tags with non-reducing linkages with the protein for measurement under
291 reduced conditions[8]. These facts highlight the generality and significance of this method for
292 protein structural studies. For application of this method to other proteins, one may concern
293 about the impact of 65% sucrose to the structure of the protein. It should be important to
294 evaluate the structure of the target protein in 65% sucrose by other methods including CD.
295 A possible future application of single-pair SAXS is in the structural study of intrinsically
296 disordered proteins (IDPs). Owing to the importance of IDPs in many biological events,
297 including liquid-liquid phase separation to form membrane-less organelles, the need for
298 information about their conformational distribution in solution is increasing. However, as with
299 multi-domain proteins, it can be difficult to adapt conventional structural analysis methods
300 because of the structural flexibility of IDPs. By combining information on the distance
301 distribution between two points in an aqueous solution with information obtained from NMR,
302 spectroscopy, and MD simulations, more detailed structural information on IDPs can be
303 obtained.
304
305

EXPERIMENTAL METHODS

Preparation of CLaNP-5

CLaNP-5 was synthesized, purified, and chelated with Lu^{3+} as described in previous reports[9,16,29].

Protein sample preparation

Escherichia coli full-length MurD (1–437) and domains 1–2 (1–302) were cloned into pGBHPS[30], expressed in *E. coli* strain BL21 (DE3), and purified as described in a previous report[9]. For SAXS measurements, MurD domains 1–2 M145C/D148C/C151A/E260C/K262C ($D12_{145\text{-}260}$) and MurD E260C/K262C/N360C/D362C ($MurD_{260–360}$) were prepared using a previously described procedure[9]. Note that $D12_{145\text{-}260}$ contains a mutation in C151A to avoid intramolecular disulfide bond formation with D148C. The CLaNP-5 tag was attached to the protein by mixing the protein and tag at a 1:2.2 ratio for 15 min on ice, followed by gel filtration. The data showed that the tags were attached to a specific position of MurD with high efficiency. Although MurD has seven cysteine residues (e.g., C20, C99, C151, C208, C227, C368, and C413), all cysteine residues have a thiol group buried in the protein and do not react with the CLaNP-5 tag[9]. To replace the protein buffer with 65% (w/v) sucrose buffer, MurD and 65% sucrose buffer were mixed in a 1:1 volume and dialyzed overnight[11]. For more accurate

contrast match, 30 uL of protein solution and 1.5 mL of 65% sucrose buffer were added to a sitting drop plate (well capacity: 1.5 mL, post capacity: 40 μl, plate dimension: approx. 15.0 cm × 10.8 cm × 2.2 cm, HAMPTON RESEACH., Ltd., Osaka, Japan) and incubated overnight.

Flow-SAXS measurement

Contrast-matched SAXS for $D12_{145\text{-}260}$ was recorded at the beamline BL-10C of the Photon Factory (PF; Tsukuba, Japan). The X-ray wavelength was 1.1 Å and the sample-detector distance was 1.0 m. Data were collected using a PILATUS 300 K detector at twenty 30-sec exposures per flow. The data from six flows were collected and averaged. A silver behenate standard was used to locate the beam center and calibrate the scattering angle values. Data reduction was performed using the SAngler software[31]. The measurements were performed in a 1.25 mm path length flow cell with fused quartz windows (2.5 mm × 6 mm × 0.02 mm, Unisoku Co., Ltd., Osaka, Japan). Silicone rubber was used to hold the windows in place. The flow rate was set to 0.33 μl min^{-1} to reduce irradiation damage. The cell temperature was set to 20°C. Buffer scattering was recorded before and after each sample. After the sample measurements, the cells were washed with a detergent solution and water.

As a reference, SAXS for D12 without lanthanide ion in 65% sucrose solution was recorded at the beamline BL-10C of the Photon Factory (PF; Tsukuba, Japan). The X-ray wavelength

342 was 1.1 Å and the sample-detector distance was 1.0 m. Data were collected using a PILATUS3
343 2M detector at twenty 30-sec exposures per flow. The data from twelve flows were collected
344 and averaged. A silver behenate standard was used to locate the beam center and calibrate the
345 scattering angle values. Data reduction was performed using the SAngler software[31]. The
346 measurements were performed in a 1.25 mm path length flow cell with fused quartz windows
347 (2.5 mm × 6 mm × 0.02 mm, Unisoku Co., Ltd., Osaka, Japan). Silicone rubber was used to
348 hold the windows in place. The flow rate was set to 0.33 μl min^{-1} to reduce irradiation damage.
349 The cell temperature was set to 20°C. Buffer scattering was recorded before and after each
350 sample. After the sample measurements, the cells were washed with a detergent solution and
351 water.

352 Contrast matched SAXS for $MurD_{260–360}$ was recorded at beamline BL-6A of the Photon
353 Factory (PF; Tsukuba, Japan). The X-ray wavelength was 1.5 Å and the sample-detector
354 distance was 1.0 m. Data were collected using a PILATUS3 1M detector with twenty 20-sec
355 exposures per flow. The data from five flows were collected and averaged. A silver behenate
356 standard was used to locate the beam center and calibrate the scattering angle values. Data
357 reduction was performed using the SAngler software[31]. The measurements were performed in
358 a 1.25 mm path length flow cell with fused quartz windows (2.5 mm × 6 mm × 0.02 mm,
359 Unisoku Co., Ltd., Osaka, Japan). Silicone rubber was used to hold the windows in place. The

360 flow rate was set to 6 μl min^{-1} and measured at 0°C to reduce irradiation damage. Buffer
361 scattering was recorded before and after each sample. After the sample measurements, the cells
362 were washed with a detergent solution and water.
363
364 *SEC-SAXS measurement*
365 SEC-SAXS for MurD and D12 was recorded at the beamline BL-10C of the Photon Factory
366 (PF; Tsukuba, Japan). The X-ray wavelength was 1.1 Å and the sample-detector distance was
367 1.0 m. Data were collected using a PILATUS 2M detector at twenty 30-sec exposures per
368 sample. A silver behenate standard was used to locate the beam center and calibrate the
369 scattering angle values. Data reduction was performed using the SAngler software[31]. The
370 measurements were performed in a 1.25-mm path length flow cell with fused quartz windows
371 (2.5 mm × 6 mm × 0.02 mm, Unisoku Co., Ltd., Osaka, Japan). Silicone rubber was used to
372 hold the windows in place. The flow rate was set at 0.05 ml min^{-1}. The cell temperature was set
373 to 20°C.
374
375 *Distance distribution analysis*
376 To extract distance distribution information from the SAXS data, the data from contrast-
377 matched SAXS were fitted with *Equation 1* using a modified version of the MATLAB program

used in a previous study[11]. The original program was used to study gold nanocrystal-labelled DNA fragments[12,13]. In the fitting of MurD data, a linear baseline correction was added. To consider the reliable range of the distance information , the SAXS curves were regenerated from the *P*(r) function. The *P*(r) function was assumed to be normal distribution. The peak top corresponded to mean (μ), and standard deviation (σ) was obtained from FWHM=2.35σ. The SAXS curve was estimated for varying μ, with the range up to ±5 Å to search for the fitted region.

SEC-MALS measurement

SEC–MALS was performed using a DAWN HELEOS8+ (Wyatt Technology Corporation, Santa Barbara, CA, USA), high-performance liquid chromatography pump LC-20AD (Shimadzu, Kyoto, Japan), refractive index detector RID-20A (Shimadzu), and UV–vis detector SPD-20A (Shimadzu), located downstream of the Shimadzu liquid chromatography system connected to a PROTEIN KW-803 gel filtration column (Cat. no. F6989103; Shodex, Tokyo, Japan). Differential RI (Shimadzu) downstream of MALS was used to determine protein concentrations. The running buffer used contained 20 mM Tris-HCl (pH 7.2) and 100 mM NaCl for D12, and 20 mM Tris-HCl (pH7.2) and 200 mM NaCl for MurD. Approximately 100 μL of the sample was injected at a flow rate of 1.0 mL min^{-1}. Data were analyzed using

ASTRA version 7.0.1 (Wyatt Technology Corporation). Molar mass analysis was also performed over half the width of the UV peak top height.

Circular dichroism spectrometer

The CD spectra were recorded using a JASCO J-1500 CD spectrometer (Tokyo, Japan) with 0.1 mm path length cuvettes at 25°C in 20 mM Tris-HCl (pH 7.2), 200 mM NaCl, and 65% (w/v) sucrose buffer. Each spectrum represents an integration of four consecutive scans from 190 to 260 nm at 1.0 nm intervals, with a scan speed of 20 nm/min. The concentrations of MurD and MurD in 65% sucrose buffer were 34 μM and 27 μM, respectively.

AUTHOR INFORMATION

Corresponding Authors

Koichiro Ishimori

Graduate School of Chemical Sciences and Engineering, Hokkaido University, Sapporo, Hokkaido 060-8628, Japan

Department of Chemistry, Faculty of Science, Hokkaido University, Sapporo, Hokkaido 060-0810, Japan

Email: koichiro@sci.hokudai.ac.jp.

Orcid https://orcid.org/0000-0002-5868-0462

Tomohide Saio

Graduate School of Medical Sciences, Tokushima University, Tokushima 770-8503, Japan

Institute of Advanced Medical Sciences, Tokushima University, Tokushima 770-8503, Japan

Fujii Memorial Institute of Medical Sciences, Institute of Advanced Medical Sciences, Tokushima University, Tokushima 770-8503, Japan

Email: saio@tokushima-u.ac.jp.

Orcid https://orcid.org/0000-0003-3639-7399

Notes

The authors declare no competing financial interest.

Supporting Information

Data for SEC-SAXS and SEC-MALS on D12 and MurD, Circular Dichroism on D12 and MurD in the absence and presence of 65% sucrose, and contrast-matched SAXS on $D12_{145\text{-}260}$ attached with the Lu^{3+} tags and D12, and Lu^{3+}–Lu^{3+} distance distributions for $D12_{145\text{-}260}$ and

431 $MurD_{260\text{-}360}$, superimposition of theoretical SAXS curves, evaluation of the reliability of
432 distance information from contrast-matched SAXS curves, and comparison of the SAXS-
433 derived distance distributions with those estimated from ESR and MD simulation.

434

435 **ACKNOWLEDGEMENTS**

436 This work was supported by funding from JSPS KAKENHI (JP21J21141 to H.K.;
437 JP18H05229, JP20H03199, JP20KK0156, JP21H05093, JP21H05094, JP22K18361, and
438 JP22H02560 to T.S.; and JP19H05769 to K.I.), MEXT Grant-in-Aid for Transformative
439 Research Areas (B) (JP21H05094 and JP21H05093 to T.S.), and JST FOREST Program
440 (JPMJFR204W to T.S.). This work was also partially supported by the Toyota Riken Scholar,
441 Takeda Science Foundation Grant, Kato Memorial Trust for Nambyo Research, Mochida
442 Memorial Foundation for Medical and Pharmaceutical Research, Naito Foundation, Yukihiko
443 Miyata Memorial Trust for ALS Research, Asahi Glass Foundation, Uehara Memorial
444 Foundation, Cannon Foundation, 2021/2022/2023 Joint Usage and Joint Research Programs,
445 Institute of Advanced Medical Sciences, Tokushima University, and Medical Research Center
446 Initiative for High Depth Omics. We also thank Dr. Hiroyuki Kumeta (Hokkaido University),
447 Dr. Noriyuki Igarashi (Photon Factory), Dr. Nobutaka Shimizu (Photon Factory), Dr. Munehiro
448 Kumashiro (Tokushima University), Dr. Yoshikazu Hattori (Tokushima University), Ms. Eri

449 Sakamoto (Tokushima University), and Ms. Kotona Kato (Tokushima University) for their
450 experimental support. Experiments at the Photon Factory were performed with the approval of
451 the Photon Factory Program Advisory Committee (Proposals 2017G566, 2019G523, and
452 2021G581 to T.S. The experiments conducted at SPring-8 (Harima, Japan) were supported by
453 the Platform Project for Supporting Drug Discovery and Life Science Research (Basis for
454 Supporting Innovative Drug Discovery and Life Science Research [BINDS]) from AMED
455 under Grant 1176 to T.S. The authors thank Dr. Nobutaka Shimizu at beamlines BL-6A, BL-
456 10C, and BL-15A2 of the Photon Factory and Dr. Takaaki Hikima at beamline BL-45XU for
457 their assistance with the SAXS measurements.

458

REFERENCES

(1) Göbl, C.; Madl, T.; Simon, B.; Sattler, M. NMR approaches for structural analysis of multidomain proteins and complexes in solution. *Prog. Nucl. Magn. Reson. Spectrosc.* **2014**, *80*, 26–63.

(2) Han, J. H.; Batey, S.; Nickson, A. A.; Teichmann, S. A.; Clarke, J. The folding and evolution of multidomain proteins. *Nat. Rev. Mol. Cell Biol.* **2007**, *8* (4), 319–330.

(3) Ma, B.; Tsai, C. J.; Haliloğlu, T.; Nussinov, R. Dynamic Allostery: Linkers are not merely flexible. *Structure* **2011**, *19* (7), 907–917.

(4) Levitt, M. Nature of the protein universe. *Proc. Natl. Acad. Sci. U. S. A.* **2009**, *106* (27), 11079–11084.

(5) Skora, L.; Mestan, J.; Fabbro, D.; Jahnke, W.; Grzesiek, S. NMR reveals the allosteric opening and closing of abelson tyrosine kinase by ATP-site and myristoyl pocket inhibitors. *Proc. Natl. Acad. Sci. U. S. A.* **2013**, *110* (47).

(6) Kurt Wüthrich, Z. NMR with proteins and nucleic acids. **1985**, 11–13.

(7) Egelman, E. H. The current revolution in Cryo-EM. *Biophys. J.* **2016**, *110* (5), 1008–1012.

(8) Saio, T.; Ishimori, K. Accelerating structural life science by paramagnetic lanthanide probe methods. *Biochim. Biophys. Acta - Gen. Subj.* **2020**, *1864* (2), 129332.

(9) Saio, T.; Ogura, K.; Kumeta, H.; Kobashigawa, Y.; Shimizu, K.; Yokochi, M.; Kodama, K.; Yamaguchi, H.; Tsujishita, H.; Inagaki, F. Ligand-driven conformational changes of MurD visualized by paramagnetic NMR. *Sci. Rep.* **2015**, *5*, 1–11.

(10) Kikhney, A. G.; Svergun, D. I. A practical guide to small angle X-ray scattering (SAXS) of flexible and intrinsically disordered proteins. *FEBS Lett*. **2015**, *589* (19), 2570–2577.

(11) Grishaev, A.; Anthis, N. J.; Clore, G. M. Contrast-matched small-angle X-ray scattering from a heavy-atom-labeled protein in structure determination: Application to a lead-substituted calmodulin-peptide complex. *J. Am. Chem. Soc*. **2012**, *134* (36), 14686–14689.

(12) Mathew-Fenn, R. S.; Das, R.; Silverman, J. A.; Walker, P. A.; Harbury, P. A. B. A molecular ruler for measuring quantitative distance distributions. *PLoS One* **2008**, *3* (10), 1–9.

(13) Mathew-Fenn, R. S.; Das, R.; Harbury, P. A. B. Remeasuring the double helix. *Science (80-.)*. **2008**, *322* (5900), 446–449.

(14) Taguchi, Y.; Saio, T.; Kohda, D. Distance distribution between two iodine atoms derived from small-angle X-ray scattering interferometry for analyzing a conformational ensemble of heavy atom-labeled small molecules. *J. Phys. Chem. Lett*. **2020**, *11* (14), 5451–5456.

(15) Popovych, N.; Tzeng, S. R.; Tonelli, M.; Ebright, R. H.; Kalodimos, C. G. Structural basis for CAMP-mediated allosteric control of the catabolite activator protein. *Proc. Natl. Acad. Sci. U. S. A*. **2009**, *106* (17), 6927–6932.

(16) Keizers, P. H. J.; Saragliadis, A.; Hiruma, Y.; Overhand, M.; Ubbink, M. Design, synthesis, and evaluation of a lanthanide chelating protein probe: CLaNP-5 yields

predictable paramagnetic effects independent of environment. *J. Am. Chem. Soc.* **2008**, *130* (44), 14802–14812.

(17) Lipfert, J.; Doniach, S. Small-angle X-ray scattering from RNA, proteins, and protein complexes. *Annu. Rev. Biophys. Biomol. Struct.* **2007**, *36*, 307–327.

(18) Smith, C. A. Structure, Function and dynamics in the mur family of bacterial cell wall ligases. *J. Mol. Biol.* **2006**, *362* (4), 640–655.

(19) Bertrand, J. A.; Auger, G.; Martin, L.; Fanchon, E.; Blanot, D.; Le Beller, D.; Van Heijenoort, J.; Dideberg, O. Determination of the MurD mechanism through crystallographic analysis of enzyme complexes. *J. Mol. Biol.* **1999**, *289* (3), 579–590.

(20) Zidar, N.; Tomašić, T.; Šink, R.; Rupnik, V.; Kovač, A.; Turk, S.; Patin, D.; Blanot, D.; Contreras Martel, C.; Dessen, A.; Müller Premru, M.; Zega, A.; Gobec, S.; Peterlin Mašič, L.; Kikelj, D. Discovery of novel 5-benzylidenerhodanine and 5-benzylidenethiazolidine-2, 4-dione inhibitors of MurD ligase. *J. Med. Chem.* **2010**, *53* (18), 6584–6594.

(21) Tomašić, T.; Šink, R.; Zidar, N.; Fic, A.; Contreras-Martel, C.; Dessen, A.; Patin, D.; Blanot, D.; Müller-Premru, M.; Gobec, S.; Zega, A.; Kikelj, D.; Mašič, L. P. Dual inhibitor of MurD and MurE ligases from Escherichia coli and Staphylococcus aureus. *ACS Med. Chem. Lett.* **2012**, *3* (8), 626–630.

(22) Bertrand, J. A.; Fanchon, E.; Martin, L.; Chantalat, L.; Auger, G.; Blanot, D.; Van Heijenoort, J.; Dideberg, O. "Open" structures of MurD: Domain movements and structural similarities with folylpolyglutamate synthetase. *J. Mol. Biol.* **2000**, *301* (5), 1257–1266.

(23) Kotnik, M.; Humljan, J.; Contreras-Martel, C.; Oblak, M.; Kristan, K.; Hervé, M.; Blanot, D.; Urleb, U.; Gobec, S.; Dessen, A.; Solmajer, T. Structural and functional characterization of enantiomeric glutamic acid derivatives as potential transition state analogue inhibitors of MurD ligase. *J. Mol. Biol.* **2007**, *370* (1), 107–115.

(24) Saio, T.; Hiramatsu, S.; Asada, M.; Nakagawa, H.; Shimizu, K.; Kumeta, H.; Nakamura, T.; Ishimori, K. Conformational ensemble of a multidomain protein explored by Gd^{3+} electron paramagnetic resonance. *Biophys. J.* **2021**, *120* (15), 2943–2951.

(25) Fleming, P. J.; Fleming, K. G. HullRad: Fast calculations of folded and disordered protein and nucleic acid hydrodynamic properties. *Biophys. J.* **2018**, *114* (4), 856–869.

(26) Grant, T. D. Ab Initio electron density determination directly from solution scattering data. *Nat. Methods* **2018**, *15* (3), 191–193.

(27) Jeffries, C. M.; Graewert, M. A.; Blanchet, C. E.; Langley, D. B.; Whitten, A. E.; Svergun, D. I. Preparing monodisperse macromolecular samples for successful biological small-angle X-ray and neutron-scattering experiments. *Nat. Protoc.* **2016**, *11* (11), 2122–2153.

(28) Nakagawa, H.; Saio, T.; Nagao, M.; Inoue, R.; Sugiyama, M.; Ajito, S.; Tominaga, T.; Kawakita, Y. Conformational dynamics of a multidomain protein by neutron scattering and computational analysis. *Biophys. J.* **2021**, *120* (16), 3341–3354.

(29) Keizers, P. H. J.; Desreux, J. F.; Overhand, M.; Ubbink, M. Increased paramagnetic effect of a lanthanide protein probe by two-point attachment. *J. Am. Chem. Soc.* **2007**, *129* (30), 9292–9293.

(30) Kobashigawa, Y.; Kumeta, H.; Ogura, K.; Inagaki, F. Attachment of an NMR-invisible solubility enhancement tag using a sortase-mediated protein ligation method. *J. Biomol. NMR* **2009**, *43* (3), 145–150.

(31) Shimizu, N.; Yatabe, K.; Nagatani, Y.; Saijyo, S.; Kosuge, T.; Igarashi, N. Software development for analysis of small-angle X-ray scattering data. *AIP Conf. Proc.* **2016**, *1741*.